Geomechanics and Engineering, *Vol. 21, No. 1 (2020) 11-21*
DOI: https://doi.org/10.12989/gae.2020.21.1.011

Bearing capacity of shallow foundations on the bilayer rock

Ana S. Alencar*[1], Rubén A. Galindo[1a] and Svetlana Melentijevic[2b]

[1]*ETSI Caminos, C. y P., Technical University of Madrid (UPM), C/ Profesor Aranguren s/n, Madrid 28040, Spain*
[2]*Faculty of Geology, Complutense University of Madrid (UCM), C/ José Antonio Nováis nº 2, Madrid 28040, Spain*

(Received June 17, 2019, Revised February 28, 2020, Accepted March 2, 2020)

Abstract. The traditional formulations for estimation of bearing capacity in rock mechanics assume a homogeneous and isotropic rock mass. However, it is common that the rock mass consists of different layers of different rock properties or of the same rock matrix with distinct geotechnical quality levels. The bearing capacity of a heterogeneous rock is estimated traditionally through the weighted average. In this paper, the solution of the weighted average is compared to the finite difference method applied to a bilayer rock mass. The influence of different parameters such as the thickness of the layers, the rock type, the uniaxial compressive strength and the overall geotechnical quality of the rock mass on the bearing capacity of a bilayer rock mass is analyzed. A parametric study by finite difference method is carried out to develop a bearing capacity factor in function of the layer thickness and the rock mass quality expressed in terms of the geological strength index, which is presented in a form of a chart. Therefore, this correlation factor allows estimating the bearing capacity of a rock mass that is formed by two layers with distinct GSI, depending on the bearing capacity of the rock mass formed only by the upper layer and considered by that way as homogenous and isotropic rock mass.

Keywords: bearing capacity; bilayer; Hoek and Brown material; finite difference method; shallow foundation; GSI

1. Introduction

For the study of the bearing capacity, several methods of analysis have been used: limit equilibrium method (Terzaghi 1943, Meyerhof 1951), slip line method (Sokolovskii 1965), limit analysis method (Sloan 1988, Sloan and Kleeman 1995), numerical method (Griffiths, 1982), stochastic approach (Shahin and Cheung 2011) and computational intelligence (Tajeri *et al.* 2015, Alavi and Sadrossadat 2016).

Traditional formulations of the bearing capacity are based on the Mohr-Coulomb parameters (cohesion and friction angle) that are very efficient in the field of soil mechanics with a linear behavior. In rock mechanics, the current methods to estimate the bearing capacity adopt the non-linear failure criterion proposed by Hoek and Brown (1980, 1997, 2002), which is applicable to the rock mass with a homogeneous and isotropic behavior.

The analytical method for shallow foundation and boundary condition that solves the internal equilibrium equations combined with the failure criterion was proposed by Serrano & Olalla (1994) and Serrano *et al.* (2000) applying the Hoek and Brown (1980) and the modified Hoek and Brown failure criterion (1997), respectively. It is based on the characteristic line method (Sokolovskii 1965), with the hypothesis of the weightless rock, strip foundation and associative flow law. The formulation of the bearing capacity proposed by Serrano *et al.* (2000) introduces a bearing capacity factor ($N_{\sigma 0}$) which makes the failure pressure proportional to the uniaxial compressive strength (UCS) of the rock.

The similar structure of the equation that relates the ultimate bearing capacity to the UCS is observed in other formulations, such as Carter and Kulhawy (1988), based on lower bound solution adopting the hypothesis of the weightless rock.

Merifield *et al.* (2006) applied the limit theorems (upper and lower bound), as an extension of the formulation developed by Lyamin and Sloan (2002a, 2002b), to determine the ultimate bearing capacity of a strip foundation on a fractured rock mass whose behavior is of the Hoek and Brown type. The authors presented the results in terms of a bearing capacity factor $N_{\sigma 0}$ and N_{σ} (considering conditions of the weightless rock mass and considering the material self-weight) in graphical form, depending mainly on the Hoek and Brown parameters (2002) m_i and GSI.

However, geotechnical engineers often deal with bilayer rock mass composed of layers of different quality. Currently the estimation of the bearing capacity of shallow foundation on rock mass formed by two-layers is performed applying the usual formulation for homogeneous and isotropic rock mass, adopting geotechnical parameters as the average weighted of the rock mass, according to the experience of each designer (Marinos and Hoek 2001, Marinos *et al.* 2006, Budetta and Nappi 2011, Özbek and Gül 2014, Marinos and Carter 2018, Santa *et al.* 2019); or through the numerical calculation that allows to model different layers

*Corresponding author, Ph.D. Student
E-mail: at.santos@alumnos.upm.es
[a]Professor
E-mail: rubenangel.galindo@upm.es
[b]Professor
E-mail: svmelent@ucm.es

http://www.techno-press.org/?journal=gae&subpage=7 ISSN: 2005-307X (Print), 2092-6219 (Online)

of the rock mass.

It is emphasized that in soil mechanics the bearing capacity of two-layered soil has been extensively studied by different authors (Meyerhof 1974, Hanna and Meyerhof 1980, Hanna 1982, 1987, Andrawes *et al.* 1996, Zhu 2004, Kuo *et al.* 2009, Kiru and Madhav 2010, Uncuoğlu E. 2015, Misir and Laman 2016) introducing different corrections factors developed both for granular and cohesive soils. Shoaei *et al.* (2012) released a review of available approaches for ultimate bearing capacity of two-layered soils, summarizing the methods applied by different authors for the estimation of the bearing capacity of a bilayer soil.

The available methods for estimating the bearing capacity of a bilayer soil usually apply one of the three methodologies: (a) providing a new bearing capacity factors to apply in the traditional Terzaghi equation (Hanna 1982); (b) proposing a new equation for the calculation of the bearing capacity that considers the soil bilayer (Hanna and Meyerhof 1980, Hanna 1982, Okamura *et al.* 1998, Farah 2004); (c) estimating a reducing factor to be applied in the bearing capacity calculated considering a homogeneous soil (Zhu 2004). Independent of the methodology the thickness of the upper layer and the footing width widely influence the bearing capacity of a bilayer soil.

Satyanarayna and Garg (1980) proposed an empirical method for the bearing capacity estimation for weighting of strength parameters, cohesion and friction (c and φ), according to the thickness of each layer. The variation of the bearing capacity of soft clay underlain by stiff clay can be estimated in charts. Hanna (1981) compared bearing capacity results obtained by experimental study with those obtained by the method proposed by Satyanarayna and Garg (1980) and observed that discrepancies ranges from 70 to 85%.

Meyerhof (1974) proposed a method to estimate the bearing capacity of a bilayer cohesionless soil formed by a weak sand layer overlying a strong layer, assuming that the bottom layer acts as a rigid base. Hanna (1982, 1987) also analyzed the bearing capacity of two-layer sand, comparing experimental results with those obtained by finite element method observing a good agreement between both methods.

Zhu (2004) proposed a chart for the estimation of a bearing capacity factor for two-layer clay soil as a function of the H/B (depth of the upper layer / width of the foundation) and the relation between the undrained cohesion of the upper and bottom layers (C1/C2). The analysis performed by Zhu (2004) will be presented in section 2 in detail considering that the results of this study are presented in the similar form.

Kuo *et al.* (2009) utilized the artificial neural network (ANN) technique for predicting the bearing capacity of strip footing on multi-layered cohesive soils.

It is emphasized that the mechanical behavior of a bilayer material is determined by the location of the weak stratum (whether being the upper layer or the bottom layer) and the thickness of the upper layer. Depending on these two variables, the size and the shape of the stress bulb change significantly as it can be seen in the schematic representation of the Fig. 1; when the bottom layer is the strong stratum, the stress bulb tends to be reduced, on the contrary, if the bottom layer is a weak layer, the depth of influence of the bulb tends to expand (Hanna 1987).

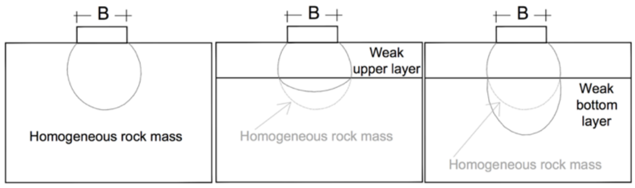

Fig. 1 Depth of influence of the stress bulb

In the present study, the bearing capacity of bilayered rock masses considering different geotechnical parameters is estimated using finite difference method in order to determine a bearing capacity factor (referred to as a Bilayer factor, B_F) for a rock mass that shows two layers with different overall geotechnical quality. Therefore, this correlation factor (B_F) allows estimating the bearing capacity of a rock mass that is formed by two layers with distinct GSI, depending on the bearing capacity of the rock mass formed only by the upper layer, considered as homogeneous and isotropic. Different thicknesses of the upper layer are analyzed, as well as the influence of the location of the weak layer (upper or bottom layer). Finally, the size and the shape of the failure wedge is analyzed considering the outputs of the displacements (horizontal and vertical) developed below the foundation obtained by the finite difference method.

2. The bearing capacity of two-layer clay soil (Zhu 2004)

The chart proposed by Zhu (2004) is described in this section, where the variation of the bearing capacity factor is represented as function of the correlation between the undrained cohesion of the upper and bottom layers (C1/C2) and the relation between the thickness of the upper layer and the foundation width (H/B) (Fig. 2).

The author proposed a bearing capacity coefficient N_c* that multiplied by the value of the undrained shear strength of the top clay layer (C1) allows to know the bearing capacity of a bilayer soil formed by two cohesive layers. The calculations were performed by the commercial finite element analysis software ABAQUS.

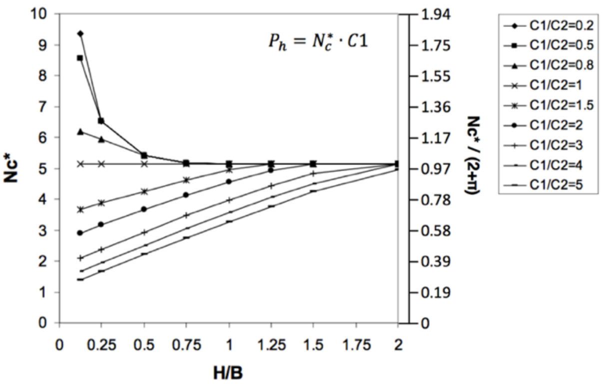

Fig. 2 Bearing capacity factor N_c* (modified from Zhu 2004)

According to the author, in Fig. 2 it can be observed that for cases where the top layer is weaker than the bottom layer ($C1/C2 < 1$), the value of N_c* decreases with the increase of H/B. For cases where the top layer is stronger than the bottom layer ($C1/C2 > 1$), the value of N_c* increases as H/B increases.

N_c* approaches $(2+\pi)$ for all cases (that is the exact solution for a strip footing over homogenous clay soil), which indicates that with the increase of the H/B the failure mechanism is limited in the top layer and the whole soil can be treated as a homogenous soil using the properties of the upper soil only. The H/B value that limits the influence of bottom layer in the bearing capacity depends on the location of the weaker layer. When the upper layer is the weaker, N_c* is greater than $2+\pi$, from H/B=0.75 the bearing capacity of bilayer soils is similar to obtained for the homogeneous case; while, in the cases that $N_c^*<(2+\pi)$ depending on the relationship between the values of C1 and C2 the bottom layer can condition the bearing capacity of bilayer soils up H/B=2. The additional vertical axes is added to the graph by dividing the values of N_c* by $(2+\pi)$ in order to obtain the convergence of all curves to the value of 1 that is further taken as a criteria for the development of the graphs presented in this paper.

3. Numerical model

Numerical calculations were developed using 2D models in the finite difference method employing commercial code FLAC, applying the plane strain condition with a symmetrical model, where only half of the strip footing is represented (Fig. 3). The boundaries of the models are located at a distance that does not interfere in the result. In all simulations the rock mass is considered weightless, and the associative flow-rule and the rough interface at the base of the foundation are adopted.

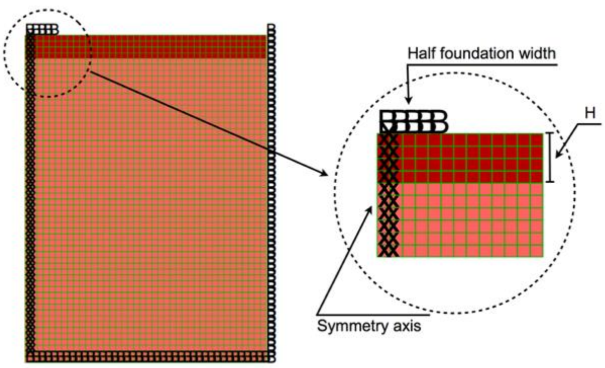

Fig. 3 2D model used

Table 1 Summary of the geotechnical parameters adopted

m_i	UCS (MPa)	GSI
5	5	10
15	30	30
30	100	50
		85

Table 2 Summary of the studied cases in function of GSI*

Cases	GSI		Rock mass
	Layer 1 (GSI_{UP})	Layer 2 (GSI_{BO})	
1	10		Homogeneous
2	30		Homogeneous
3	50		Homogeneous
4	85		Homogeneous
5	10	30	Bilayer
6	30	10	Bilayer
7	10	50	Bilayer
8	50	10	Bilayer
9	10	85	Bilayer
10	85	10	Bilayer
11	30	50	Bilayer
12	50	30	Bilayer
13	30	85	Bilayer
14	85	30	Bilayer
15	50	85	Bilayer
16	85	50	Bilayer

*All hypothesis are calculated for the nine combinations of m_i and UCS from Table 1

Table 3 Summary of the studied cases in function of GSI*

	Distance from the foundation level to the second layer (H) (Fig. 4)
Weak upper layer	0.33B
	0.44B
	0.67B
	B
	1.44B
	3B
Weak bottom layer	0.44B
	B
	1.44B
	2B
	3B

*All hypothesis are calculated for the nine combinations of m_i and UCS from Table 1

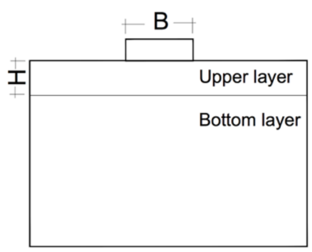

Fig. 4 Scheme of bilayer model

Numerically it is assumed that the ultimate bearing capacity is reached when the continuous medium does not admit more load because an internal failure mechanism is formed. The load is applied through velocity increments, and the ultimate bearing capacity is known from the relation between stresses and displacements of one of the nodes (in this case the central node of the foundation is considered).

A convergence study is carried out as well, consisting in analyzing values of the ultimate bearing capacity obtained under different increments of the velocity that is used, with the decrease in the value of velocity increments, and the result converges towards the final value by the upper limit in the theoretical method. For each case with a different combination of geometrical and geotechnical parameters, a convergence study is carried out with different values of velocity increments.

The study analyzes a rock mass with two layers with different values of GSI (Geological Strength Index); adopting that both layers present the same m_i and UCS. Table 1 summarizes the range of values of the geotechnical parameters applied in the models and it can be seen that a wide variety of types and states of rock masses are covered.

Based on four GSI values from Table 1, sixteen types of rock mass listed in Table 2 are generated for the numerical analysis considering. The bilayer cases are calculated considering eleven different locations of the weak layer defined in function of the width of foundation (Table 3). All hypothesis listed in Table 2 and 3 are calculated for the nine combinations of m_i and UCS from Table 1. For the hypothesis of the weak layer in the upper surface zone more cases are analysed due to the exponential variation of the bearing capacity observed in such cases.

The footing width (B) theoretically does not affect the bearing capacity, once the material self-weight is not considered in the model. Therefore, the adoption of other values for the foundation width is only a change of scale. The model adopting the footing width (B) of 4.5 m is analyzed in this paper.

To check the results and validate the charts, due to the variation observed in the trend of the results for the values of GSI (Table 2), some additional calculation models for specific charts presented further in section 4.2.1 are also performed with the following GSI values 12, 15, 17, 20, 35, 40, 45, 60 and 70 whose results are discussed further.

4. Analysis and results

4.1 Comparison of results obtained with "weighted average" and a bilayer model performed by FDM

In this study, three different methodologies were used for the estimation and comparison of the bearing capacity of a bilayered rock mass by numerical method (finite difference method applying the commercial code FLAC).

It is important to note that there is a thickness of the upper layer that makes that the bottom layer does not affect the bearing capacity, it is the H_{max}. It varies in each example and it is estimated according to the stress bulb obtained by method (3). Using the value of H and the H_{max} in the methods (1) and (2) the proportion of each layer (GSI) in the H_{max} is determined.

In the method (1) used, P_{hPRO}, the bearing capacity of each level is calculated independently as if each layer forms a homogeneous and isotropic rock mass, and then the global bearing capacity is estimated by weighting the bearing capacity of each layer by the proportion of thickness each layer in the H_{max}.

In the method (2), P_{hGSI}, it is adopted an average weighted value of GSI for the rock mass, that is determined according to the proportion of thickness of each stratum in the H_{max}.

In the method (3), P_{hB}, it is used a model with two different layers.

Table 4 Example with GSI = 10/30

	GSI_{UP} = 10 / GSI_{BO} = 30 (H_{max}=1.44B)*				GSI_{UP} = 30 / GSI_{BO} = 10 (H_{max}=2B)*		
H/B	0.33	0.44	0.67	1	0.44	1	1.44
H/H_{max} (%)	23	31	47	69	22	50	72
GSI weighted average (Method 2)	25.4	23.9	20.7	16.1	14.4	20.0	24.4
	Ultimate Bearing Capacity (MPa)						
Method 1 (P_{hPRO})	5.99	5.53	4.57	3.19	2.68	4.36	5.69
Method 2 (P_{hGSI})	5.58	5.05	4.01	2.70	2.28	3.8	5.22
Method 3 (P_{hB})	3.31	2.39	1.71	1.41	2.55	4.58	6.57

*The value of H_{max} can be observed in Fig. 5, corresponding to the thickness where the bottom layer does not affect the bearing capacity

Table 5 Example with GSI = 30/50

	GSI_{UP} = 30 / GSI_{BO} = 50 (H_{max}=1B)*			GSI_{UP} = 50 / GSI_{BO} = 30 (H_{max}=1.44B)*	
H/B	0.33	0.44	0.67	0.44	1
H/H_{max} (%)	33	44	67	31	69
GSI weighted average (Method 2)	43.4	41.2	36.6	36.1	43.9
	Ultimate Bearing Capacity (MPa)				
Method 1 (P_{hPRO})	15.58	14.23	11.42	11.12	15.88
Method 2 (P_{hGSI})	14.55	13.11	10.48	10.2	14.9
Method 3 (P_{hB})	13.6	11.55	9.79	10.79	15.45

*The value of H_{max} can be observed in Fig. 5, corresponding to the thickness where the bottom layer does not affect the bearing capacity

Table 6 Example with GSI = 30/85

	GSI_{UP} = 30 / GSI_{BO} = 85 (H_{max}=1.44B)*				GSI_{UP} = 85 / GSI_{BO} = 30 (H_{max}=2B)*		
H/B	0.33	0.44	1	1.44	0.44	1	1.44
H/H_{max} (%)	78	50	28	69	22	50	72
GSI weighted average (Method 2)	72.4	68.2	58.4	46.8	42.1	57.5	69.6
	Ultimate Bearing Capacity (MPa)						
Method 1 (P_{hPRO})	72.5	66	52.5	33.2	25.9	49.6	68.2
Method 2 (P_{hGSI})	52.6	43.75	29.77	17.02	13.7	27.4	46.54
Method 3 (P_{hB})	15.25	11.60	8.80	7.55	21.94	45.3	67

*The value of H_{max} can be observed in Fig. 5, corresponding to the thickness where the bottom layer does not affect the bearing capacity

The first two methods can be adopted as well in the application of the usual analytical formulations that consider the rock mass as homogenous and isotropic of the Hoek and Brown failure type.

It is important to note that those methodologies (1 and 2) does not consider which layer is on the surface, although the upper layer is the one that most influences the bearing capacity.

Tables 4, 5 and 6 show the results of bearing capacity obtained by three methods previously described (method 1, method 2 and method 3) for six examples that were studied according to the parameters given in Table 1. In these six examples the geotechnical parameters adopted are m_i=5, UCS=30MPa and the following combinations of GSI_{UP}/GSI_{BO} 10/30 and 30/10; 30/50 and 50/30; 30/85 and 85/30 (Tables 4, 5 and 6, respectively). It is recalled that all cases are calculated adopting weightless rock mass, associative flow rule, rough foundation base interface and the width of the strip foundation B=4.5 m as previously described in section 3.

According to the results obtained and presented in Table 4, Table 5 and Table 6 there are great differences between values of bearing capacity obtained by three methods previously described. When the upper layer is a weaker stratum, method 1 and 2 (P_{hPRO} and P_{hGSI}) overestimate the bearing capacity. This happens because these methods do not take into account the locations of the weak and strong layer, and as outlined previously, the upper layer is one that most influences the bearing capacity. It can also be observed that the greater the GSI difference between the layers, the variation between values of the bearing capacity obtained by the three different methods (P_{hB}, P_{hGSI} and P_{hPRO}) is also higher. However, the value obtained by method 2 (P_{hGSI}) is more similar to value obtained by method 3 (P_{hB}) than the results obtained for method 1 (P_{hPRO}).

In the cases that the upper layer is stronger than the bottom layer, it can be observed that the results from method 2 (P_{hGSI}) is lower than those obtained by method 3 (P_{hB}); and the method 1 (P_{hPRO}) is very close to method 3 (P_{hB}). It is concluded that if the upper layer is the most competent, the estimation by the "weighted average" is quite acceptable. However, in the cases where the upper layer is the weak stratum, the variation between the results of the methods is very significant, which is explained by not considering the location of both layers and being the upper layer the one that most conditions the bearing capacity.

Due to the variability of the results of the bearing capacity estimated considering the bilayer rock mass as a homogeneous and isotropic material, the necessity to develop a method that allows to calculate the bearing capacity of shallow foundation on a bilayer rock mass is evident.

4.2 FDM analysis

Taking into account that available methodologies for the bearing capacity estimation of a shallow foundation do not present a satisfactory result for cases of a bilayer rock mass, and the great development of different methodologies for

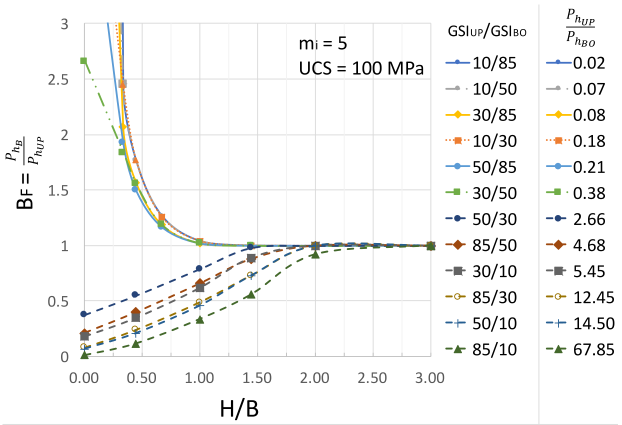

Fig. 5 Correlation between H/B and B_F as function of GSI_{UP}/GSI_{BO} and $(\frac{P_{h_{UP}}}{P_{h_{BO}}})$

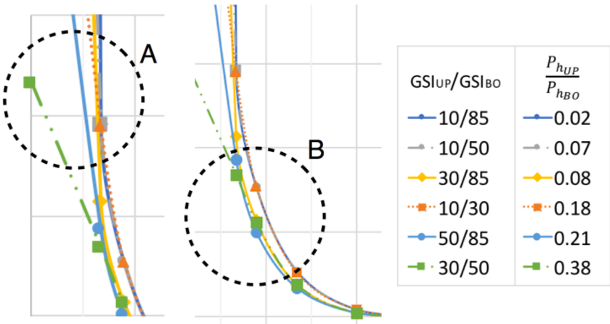

Fig. 6 Detail of two zones from Fig. 5

the consideration of the influence of two layer in the bearing capacity in the field of soil mechanics, in this paper a methodology is proposed to estimate the bearing capacity of a shallow foundation on rock mass formed by two layers with different GSI value depending on the bearing capacity of the rock mass in function of only GSI of the upper layer (GSI_{UP}). The values of the rock type (m_i) and UCS of the bilayer rock mass are maintained the same for the upper and bottom layers.

In this Section the results obtained by method 3 described in Section 4.1 that is defined as FDM model.

4.2.1 Results

The coefficient B_F is introduced and is defined as the ratio between the bearing capacity of the bilayer rock mass (P_{hB}) and the bearing capacity of the homogenous and isotropic model formed by the upper layer (P_{hUP}). Therefore, when B_F = 1 the bearing capacity of the bilayer rock mass is equal to the bearing capacity of the homogenous and isotropic material formed by the upper layer ($P_{hB} = P_{hUP}$), in this case it means that the bottom layer is located at a distance that does not interfere in the bearing capacity. When $B_F \geq 1$, it is known that the weak layer is the upper layer, because it means that the value of P_{hB} is higher than the obtained one for the upper layer (P_{hUP}). And finally, $B_F \leq 1$ is associated with the cases that the P_{hB} is less than P_{hUP}, so the bottom layer is the weak stratum.

To represent the value of B_F when the thickness of the upper layer (H) is so small that the relation H/B≈0 and the

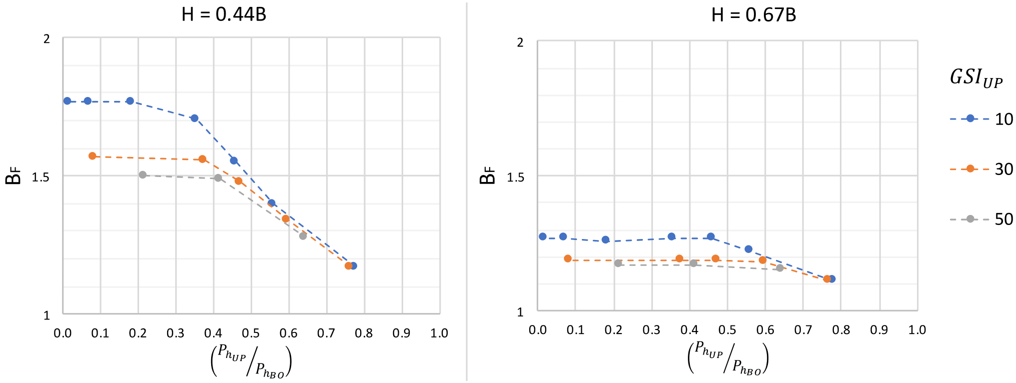

Fig. 7 B_F as function of $\left(\frac{P_{h_{UP}}}{P_{h_{BO}}}\right)$

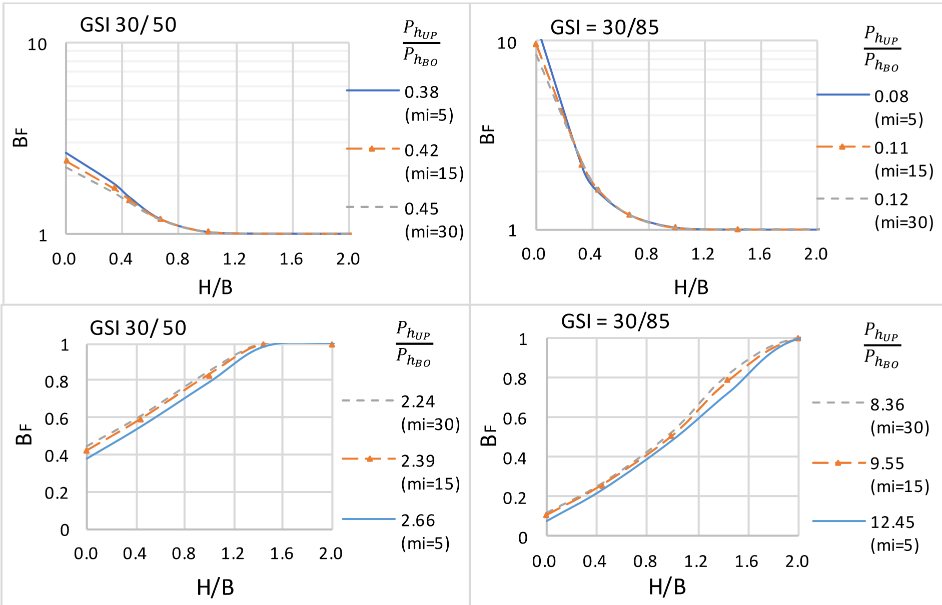

Fig. 8 Correlation between H/B and B_F as function of m_i

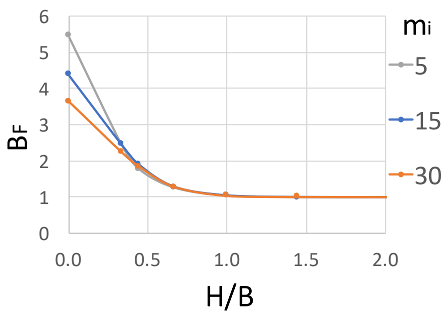

Fig. 9 Correlation between H/B and B_F as function of m_i, for UCS =30MPa and GSI= 10/30

rock mass is almost homogenous and isotropic, the maximum variation that occurs between the bearing capacity of two layers is considered $\left(\frac{P_{h_{UP}}}{P_{h_{BO}}}\right)$ (P_{hBO} and P_{hUP}, bottom and upper layer respectively). From that point (H/B≈0) to the first point numerically calculated (H/B=0.33) a line should be drawn; in Fig. 5 it can be observed that the path of the lines between H/B = 0 and the first point obtained by the numerical model is well adjusted with other points calculated numerically.

Table 7 Results of the bearing capacity of a homogeneous rock mass

GSI	UCS (MPa)	
	5	100
	Ultimate bearing capacity (MPa)	
10	0.225	4.51
30	1.23	24.57
50	3.28	65.46
85	15.35	306.55

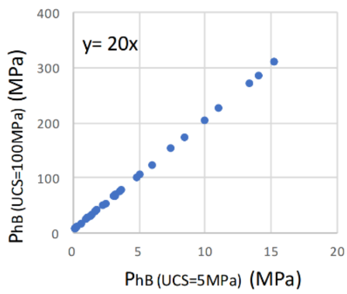

Fig. 10 Correlation between the bilayer rock mass bearing capacity depending on the UCS

The results obtained can be expressed according to two aspects: (1) the GSI values of the two layers (GSI_{UP}/GSI_{BO}); (2) the ratio between the bearing capacity of the layers ($\frac{P_{h_{UP}}}{P_{h_{BO}}}$). In the legend (1) ($GSI_{UP}/GSI_{BO}$) the relationship depends on the absolute values of the GSI, not the ratio between the GSI values; while the legend (2) represents the relationship between values of the bearing capacity obtained for the upper (Ph_{UP}) and bottom (Ph_{BO}) layer and not the absolute value. In Fig. 5 the results are presented for the value of B_F determined for the bearing capacity obtained for the case with $m_i = 5$ and UCS = 100 MPa, showing two different path of the relationship for $B_F<1$ and $B_F>1$.

For $B_F < 1$ the most generic way to represent the relationship is based on the relation between the values of the bearing capacity. It is observed that the trend is almost linear, and it is independent of the GSI value. It can be observed that the smaller the difference between the bearing capacity of the two layers the curves are closest to $B_F = 1$ (Fig. 5). It is recalled that if the two layers present the same GSI it is the homogeneous case and $B_F = 1$.

However, for $B_F > 1$, the behavior is exponential and some curves with a very similar value of ($\frac{P_{h_{UP}}}{P_{h_{BO}}}$) follow different trajectories in the graph presented in Fig. 5 (i.e., $\frac{P_{h_{UP}}}{P_{h_{BO}}}$) = 0.07 (10/50) and ($\frac{P_{h_{UP}}}{P_{h_{BO}}}$) = 0.08 (35/85)). In Fig. 6 a detail of two different parts of the Fig. 5 is presented for $B_F > 1$. It can be seen inside the circle A, that there is a zone of very low values of H/B (H/B < 0.4), that the curves are moving away from $B_F = 1$ with the decrease of the value of ($\frac{P_{h_{UP}}}{P_{h_{BO}}}$) (the same trend is observed in case of $B_F < 1$). Inside the circle B (Fig. 6), it is noted that six curves overlap and convert into three curves again, and that the value of the ratio ($\frac{P_{h_{UP}}}{P_{h_{BO}}}$) does not define the location of each of the curves. In this case, the determining factor is the GSI value of the upper layer (GSI_{UP}). This happens because, as it can be seen in Fig. 7, depending on the value of the GSI_{UP} below a ratio of ($\frac{P_{h_{UP}}}{P_{h_{BO}}}$), the value of B_F becomes constant, and all the cases studied (Table 2) are in this part of the graph. For the development of these complementary graphs (Fig. 7) other cases with distinct GSI values were analyzed (i.e. 12, 15, 17, 20, 35, 40, 45, 60 and 70) from those originally planned in Table 1 (10, 30, 50, 85) and applied only for the bottom layer. The two additional cases of H/B, in which B_F has a greater variation range are analyzed (H/B = 0.44 and 0.67) (according to observed in Fig. 5). From Fig. 7, it can be concluded that the higher the H/B value, the lower the variability of B_F.

Analyzing a depth of H = 0.44B in Fig. 7, it can be concluded that if the condition of $\frac{P_{h_{UP}}}{P_{h_{BO}}} < 0.3$ complies, B_F is constant and dependent on GSI_{UP}. Due to the fact that the bearing capacity increases exponentially with the increase in the GSI value, the relation $\frac{P_{h_{UP}}}{P_{h_{BO}}} < 0.3$ is fulfilled for quite similar GSI value, such as the case with the upper layer $GSI_{UP} = 10$ and the bottom $GSI_{BO} \geq 20$; $GSI_{UP} = 30$ and $GSI_{BO} \geq 50$; or $GSI_{UP} = 50$ and $GSI_{BO} \geq 70$.

Fig. 5 shows also that when the upper layer is weak, the bottom layer stops to influence the bearing capacity when H/B > 1; while in cases that the upper layer is more resistant for H/B = 1 the bottom layer still conditions the result of the bearing capacity. This is justified because the stress bulb tends to extend from a more resistant layer to a weaker one, reaching greater depth, confirming the theory represented in Fig. 1.

As it was possible to verify, the structure of Fig. 2 (modified from Zhu 2004) is the same as the adopted one in the present study, where the bearing capacity of a shallow foundation on a bilayer rock mass is estimated multiplying the factor B_F by the bearing capacity of the upper layer considering the rock mass as homogeneous and isotropic. Even so, in the case of N_c* as it is multiplied by the cohesion of the upper layer, to know its bearing capacity, it is necessary to apply a coefficient (in case 5.146), and for that reason the curves of the chart of Zhu (2004) converge for 5.146 and not for 1 as in the case of B_F (the right axis of Fig. 2 was modified to facilitate comparison with B_F presented in Fig. 5).

It can be observed that the curves trend of Fig. 2 are similar to that obtained in the present study summarized in Fig. 5. For the cases with the weak upper layer (top of the charts) an exponential tendency is observed that converges to the result of the bearing capacity of a homogeneous and isotropic rock mass when the bottom layer is located at a depth greater than 1B. The part of the graphs below the B_F=1 shows a more linear trend, that only converges to the result of the homogeneous and isotropic case when the thickness of the upper layer is of the order of 2B (Fig. 5).

In relation to the N_c* value, it is observed that the percentage ratio of this coefficient is in the same order of magnitude as that obtained in the present study. In both graphs (Fig. 5 and Fig. 2) the mean values of increase and reduction of the bearing capacity, go from a reduction of $0.2{*}P_{hUP}$, until the value of P_{hUP} up to 100% (values outside these ranges are found for very low values of H/B or associated with extreme values of correlation between the two layers).

On the other hand, knowing the shape of the curves (exponential for $B_F > 1$ and linear for $B_F <1$) in a chart B_F-H/B (Fig. 5) (a function of the relation between the bearing capacity of both layers or the GSI of the upper layer), a sensitivity study is carried out to know qualitatively and quantitatively how other geotechnical parameters influence the value of B_F.

4.2.2 Sensitivity analysis

In the numerical models three types of rock mass (m_i) are used for the study (Table 1). In Fig. 8 (which represents the cases of GSI 30/50 and 30/85) each one of the curves is associated with a value of mi. It can be noted that the curves are significantly distanced for $B_F > 1$ and H/B < 0.4, which means that the rock type only influences the B_F value for very low relation of H/B. It is emphasized that this happens because the rock type (m_i) significantly influences the relation between the results of the bearing capacity $\frac{P_{h_{UP}}}{P_{h_{BO}}}$ and in this area of the graph this relationship is determinant

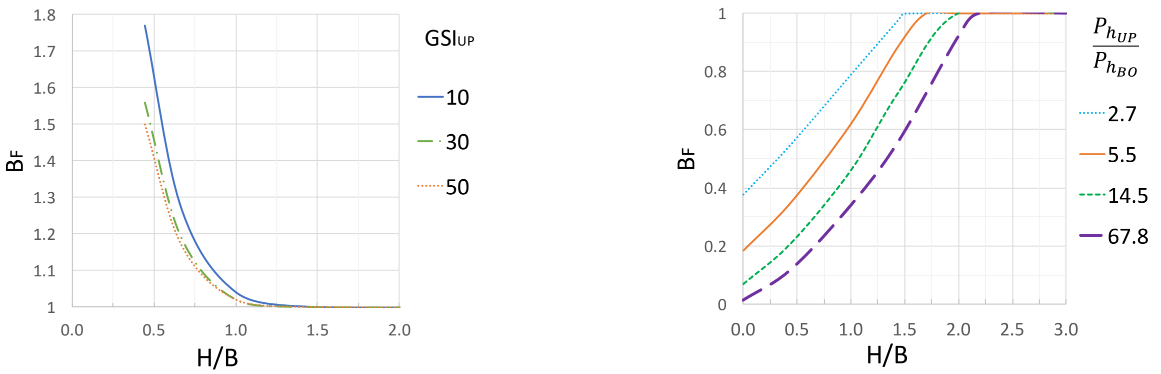

(a) $B_F > 1$ (b) $B_F < 1$

Fig. 11 Correlation between B_F and H/B

Table 8 Examples of B_F application

Example	GSI_{UP}	GSI_{BO}	H/B	P_{hUP} (MPa) (Serrano *et al.* 2000)	P_{hBO} (MPa) (Serrano *et al.* 2000)	$\frac{P_{h_{UP}}}{P_{h_{BO}}}$	B_F	P_{hB} (MPa) (B_F and Serrano *et al.* 2000)
1	30	40	0.44	1.19	2.01	0.59	1.34	1.59
2	30	50	0.2	1.19	3.24	0.37	2.19	2.61
3	30	50	0.6	1.19	3.24	0.37	1.28	1.52
4	50	30	1	3.24	1.19	2.72	0.8	2.59

in the value of B_F.

According to the results presented in Fig. 9, with the decrease of the m_i value, the value of B_F tends to be greater, under equal conditions, comparing cases with different m_i values associated to a low ($m_i = 5$) and high ($m_i = 30$) value, the variation of the B_F can exceed 50% (Fig. 9). It is also observed that the value of m_i does not have an influence on results for H/B>0.4.

Regarding the influence of the UCS on the bearing capacity of shallow foundation on rock mass, it is important to emphasize that the general formulations for the calculation of bearing capacity in rock mechanics (Carter and Kulhawy 1988, Serrano *et al.* 2000, Merifield 2006) usually applies a bearing capacity factor (N_σ) to the uniaxial compressive strength of the rock, being the bearing capacity expressed as UCS*N_σ.

To obtain the value of B_F the result of the bilayer model (P_{hB}) is divided by the result of homogeneous model formed only by the upper rock layer (P_{hUP}), presenting both models the same UCS, and therefore B_F is estimated as function of N_σ that is independent of the UCS value. Considering that, the variation of the UCS influence the bearing capacity, however it does not influence the value of B_F (Fig. 10).

Therefore, from Table 7 can be concluded that the results obtained in the case of $m_i = 5$ and UCS = 100 MPa are 20 times greater than those estimated with UCS = 5 MPa for the same rock type ($m_i = 5$). In Fig. 10 each point represents the results of the bearing capacity of bilayer model where only the value of the UCS changes (it is recalled that in the studied bilayer model the UCS value is the same in the both upper and bottom layer), so each point is associated with a combination of GSI_{UP} and GSI_{BO}, H/B and $m_i = 5$. Fig. 10 shows that in the bilayer model the bearing capacity is directly proportional to the UCS, and according to the results obtained the coefficient B_F is not influenced by the value of the UCS.

4.2.3 Bilayer factor (B_F)

According to the analysis in the previous section, UCS does not affect the B_F coefficient; the rock type (m_i) slightly modifies the value of B_F when $B_F > 1$ and H/B < 0.4. Under hypotheses previously stated the charts for the estimation of B_F are proposed in Fig. 11.

Fig. 11(a) is developed assuming $\frac{P_{h_{UP}}}{P_{h_{BO}}} < 0.3$ for B_F>1 and three different values of GSI_{UP} (10, 30, 50). This Fig. 11a is valid as well for values of $\frac{P_{h_{UP}}}{P_{h_{BO}}} > 0.3$ according to Fig. 7 depending on the GSI_{UP} and the H/B relation, because the chart of B_F-H/B can be used as long as the value of B_F is already in the horizontal part represented in Fig. 7. In the cases that $\frac{P_{h_{UP}}}{P_{h_{BO}}} > 0.3$, in a conservative way, it can be assumed that the bearing capacity of the bilayer rock mass is equal to P_{hUP} or interpolate the B_F from Fig. 7.

It is emphasized that for $B_F = 1$ the bottom layer does not influence the bearing capacity; for $B_F > 1$ the upper layer is the weak layer and for $B_F < 1$ the bottom layer is the weak stratum, according to the analysis made in section 4.2.

In Fig. 11 the value of B_F can be estimated by three different ways depending on the area of the graph where is located:

- $B_F < 1$: knowing the relation between P_{hUP} and P_{hBO}, the curve that best fit is found or interpolated (Fig. 11(b)).
- $B_F > 1$ and H/B < 0.4: B_F values also depend on the rock type (m_i), it is recommended to draw a straight line between the two points, H/B = 0 (estimated by the relation of $\frac{P_{h_{UP}}}{P_{h_{BO}}}$) and the first correspondent point in the curve represented in the Fig. 11(a);

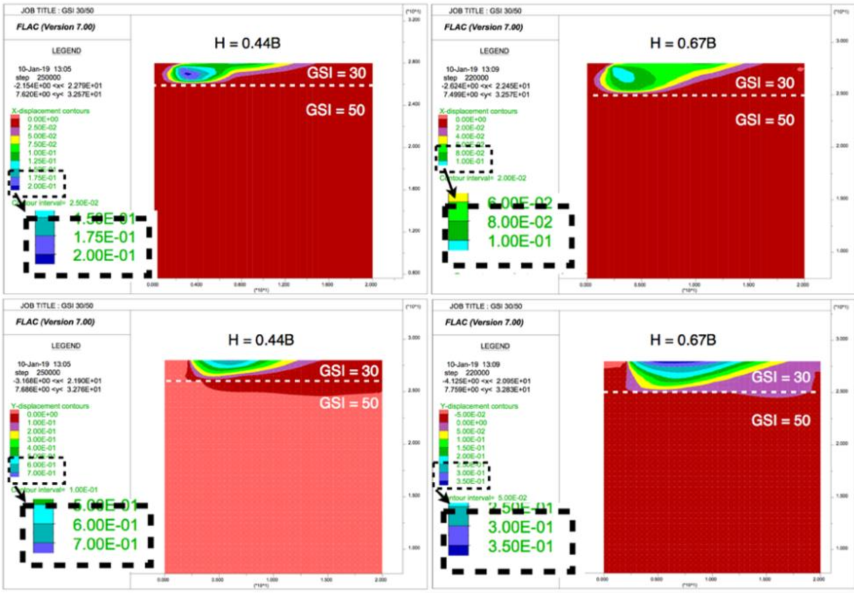

Fig. 12 The variation of the horizontal and vertical displacements obtained by FDM under the foundation (weak upper layer) (m_i = 5 and UCS = 30 MPa)

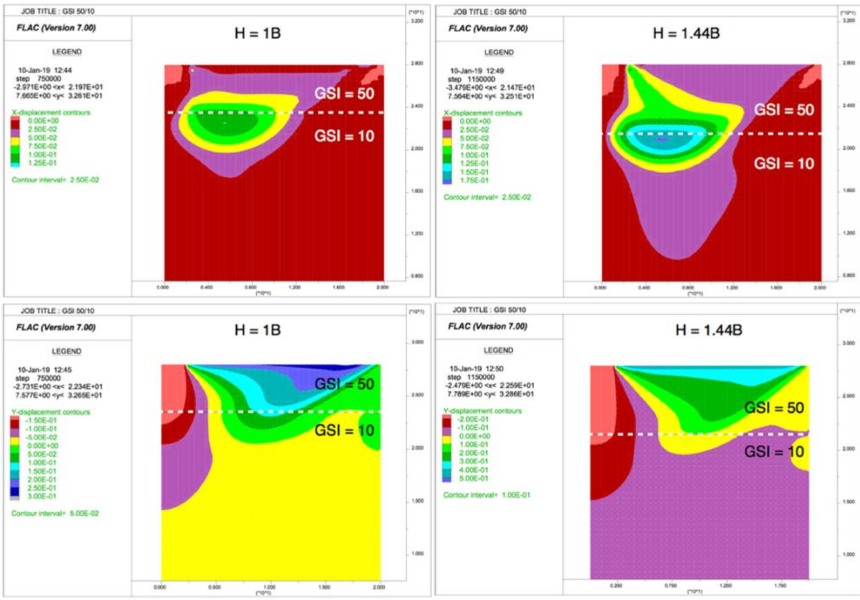

Fig. 13 The variation of horizontal and vertical displacements obtained by FDM under the foundation (weak bottom layer) (m_i=5 and UCS=30 MPa)

- $B_F > 1$ and $H/B > 0.4$: B_F is defined depending on the GSI_{UP} (Fig. 11(a)).

4.2.4 Application examples

For the estimation of the bearing capacity of shallow foundation on bilayer rock mass using the B_F factor is necessary to calculate the bearing capacity of each layer, assuming the rock mass as homogeneous and isotropic, through the method that the designer considers most appropriate (such as Carter and Kulhawy 1988, Serrano *et al.* 2000, Merifield *et al.* 2006).

Table 8 summarizes the results of four studied cases. The bearing capacity of the following examples is calculated by the method proposed by Serrano *et al.* (2000), adopting m_i = 5 and UCS = 5 MPa.

In example 1, the relation between P_{hUP} and P_{hBO} is equal to 0.59 which means that the graph of B_F-H/B proposed in Fig. 11 should not be used. In these cases, the approximate value of B_F can be estimated using Fig. 7.

In example 2, for the value of H/B = 0.2 the value of B_F is not defined in Fig. 11 because it depends on the rock type. On the other hand, $\frac{P_{h_{UP}}}{P_{h_{BO}}} = 0.37$, however, it can be observed in Fig. 7 that for GSI_{UP} = 30 for this ratio of bearing capacity $\frac{P_{h_{UP}}}{P_{h_{BO}}}$ the value of B_F is already constant. So, to know the value of B_F in this case, it is necessary to define the maximum value of B_F (H/B ≈ 0, $\frac{P_{h_{UP}}}{P_{h_{BO}}} = 2.72$), join it with the first point of the corresponding curve in Fig. 11 (H/B = 0.44, B_F = 1.56), and linearly interpolate the value of B_F; with this methodology it is obtained that H/B = 0.2 and B_F = 2.19.

In examples 3 and 4, Fig. 11 can be applied directly. In example 3, using Fig. 11(a), once $GSI_{UP} < GSI_{BO}$, therefore B_F is dependent on the value of GSI_{UP}. In example 4, $GSI_{UP} > GSI_{BO}$, Fig. 11(b) is applied, knowing the B_F value as a function of the ratio $\frac{P_{h_{UP}}}{P_{h_{BO}}}$.

4.2.5 Displacement analysis

In the numerical calculation to estimate the bearing capacity, a stress path is formed until the failure is reached, taking into account the whole wedge of the ground below the foundation. Therefore, the graphic output of the displacements, both horizontal and vertical, developed below the foundation are used to understand how the failure mechanism affects the results.

Fig. 12 shows the displacements contours (horizontal and vertical) for two cases for which the upper layer is the weak stratum, being the difference between case the thickness of the first layer (H=0.44B and H=0.67B). It can be observed that both displacements are concentrated in the upper layer. It can also be observed in Fig. 12 that the value of maximum displacements (vertical and horizontal) are associated with the thickness of the upper layer (H), being greater for smaller values of H.

On the other hand, in Fig. 13 two cases are represented in which the bottom layer is weak for the H = 1B and H = 1.44B. It can be seen that the bulb of maximum horizontal displacements is located in the area under the contact between the two layers, showing the maximum horizontal displacement in the bottom layer.

In addition, it is also observed that the displacements reach greater depths for cases presented in Fig. 12 and Fig. 13 compared to homogeneous case presented in Fig. 14 considering the value of GSI as of the upper layer in the bilayer model.

Comparing displacements presented in Fig. 12, Fig. 13 and Fig. 14, it can be concluded that the location of the stress in soils and in rocks coincide, therefore according to the theory of soil mechanics (Fig. 1) the stress bulb deepens when the weaker layer is the bottom one (Fig. 13).

5. Conclusions

Taking into account the results of bearing capacity of a two-layer rock mass described in previous sections obtained through the finite difference method under the assumptions of plane strain condition, associated flow rule, rough interface at the foundation base and weightless rock mass, applying the same UCS value and the rock type in the upper and bottom layer of the bilayer model, the following can be concluded:

- The UCS does not influence the value of B_F, because this parameter influences the bearing capacity of each layer in the same proportion.
- The rock type (m_i) conditions the value of B_F only if H/B < 0.4 and B_F > 1.
- For the B_F = 1 the bottom layer does not influence the bearing capacity (representing homogeneous and isotropic rock mass); for B_F > 1 the upper layer is weak (the stress bulb is reduced); and for B_F < 1 the bottom layer is weak (the stress bulb tend to expand) (Fig. 1).
- The curves show an exponential tendency for B_F > 1 (approximately for H/B > 1) and linear for B_F < 1 (approximately for the range of H/B between 1.5 and 2.2) in the chart of B_F-H/B (Fig. 11), and they are based on the relation of the bearing capacity of the layers ($\frac{P_{h_{UP}}}{P_{h_{BO}}}$) or the GSI value of the upper layer (GSI_{UP}).
- When the upper layer is weak (B_F > 1), the bottom layer does not affect the bearing capacity when approximately H/B > 1; while for the cases when the upper layer is more resistant (B_F < 1) for H/B = 1 the bottom layer still conditions the result of bearing capacity. This is influenced by the stress bulb that tend to extend when going from a more resistant layer to a weaker one.
- In the cases that the upper layer is weaker than the bottom one ($GSI_{UP} < GSI_{BO}$), the displacements (horizontal and vertical) are located in the upper layer. When the upper layer is more resistant ($GSI_{UP} > GSI_{BO}$), the maximum horizontal displacements are displaced for the bottom layer, reaching greater depths.
- When the upper layer is more resistant ($GSI_{UP} > GSI_{BO}$), the estimation of the bearing capacity using the "weighted average" is quite satisfactory. However, in the cases that the upper layer is weak ($GSI_{UP} < GSI_{BO}$), the variation among the methods is quite significant, due to the fact that the location of the layers is not considered, and it is the upper layer that most influences the bearing capacity.
- The shape of the curves in the chart B_F-H/B is very similar to the ones presented in graphic proposed by Zhu (2004) for two-layer clay whose parameters are defined by the undrained shear strength. It can be observed an exponential trend when the upper layer is weak ($GSI_{UP} < GSI_{BO}$; C1 < C2) and an almost linear trend when the strongest layer is on the surface ($GSI_{UP} > GSI_{BO}$; Cu1 > Cu2), both for the soil and rock material.

Acknowledgments

The research described in this paper was financially supported by the José Entrecanales Ibarra Foundation.

References

Alavi, A.H. and Sadrossadat, E. (2016), "New design equations for estimation of ultimate bearing capacity of shallow foundations resting on rock masses", *Geosci. Front.*, **7**(1), 91-99, https://doi.org/10.1016/j.gsf.2014.12.005.

Andrawes, K.Z., Al-Omari, R.R. and Kirkpatrick, W.M. (1996), "Bearing capacity of a strip foundation on a sand layer overlying a smooth rigid stratum", *Geotech. Geol. Eng.*, **14**(3), 227-236. https://doi.org/10.1007/BF00452949.

Budetta, P. and Napp,i M. (2011), "Heterogeneous rock mass classification by means of the geological strength index: The San Mauro formation (Cilento, Italy)", *Bull. Eng. Geol.*

Environ., **70**(4), 585-593. https://doi.org/10.1007/s10064-011-0351-1.

Carter, J.P. and Kulhawy, F.H. (1988), "Analysis and design of foundations socketed into rock", Report No. EL-5918, Empire State Electric Engineering Research Corporation and Electric Power Research Institute, New York, U.S.A.

Farah, C.A. (2004), "Ultimate bearing capacity of shallow foundations on layered soils", M.Sc Thesis, Concordia University, Montreal, Quebec, Canada

Griffiths, D.V. (1982), "Computation of bearing capacity factors using finite elements", *Geotechnique*, **32**(3), 195-202. https://doi.org/10.1680/geot.1982.32.3.195.

Hanna, A.M. (1981), "Experimental study on footings in layered soil", *J. Geotech. Eng. Div*., **107**(8), 1113-1127.

Hanna, A.M. (1982), "Bearing capacity of foundations on a weak sand layer overlaying a strong deposit", *Can. Geotech. J*., **19**(3), 392-396. https://doi.org/10.1139/t82-043.

Hanna, A.M. (1987), "Finite element analysis of footings on layered soils", *Math. Modell*., **9**(11), 813-819. https://doi.org/10.1016/0270-0255(87)90501-X.

Hanna, A.M. and Meyerhof, G.G. (1980), "Design charts for ultimate bearing capacity of foundations on sand overlying soft clay", *Can. Geotech. J*., **17**(2), 300-303. https://doi.org/10.1139/t80-030.

Hoek, E. and Brown, E.T. (1980), "Empirical strength criterion for rock masses", *J. Geotech. Eng. Div*., **106**(9), 1013-1035.

Hoek, E. and Brown, E.T. (1997), "Practical estimates of rock mass strength", *Int. J. Rock Mech. Min. Sci*., **34**(8), 1165-1186. https://doi.org/10.1016/S1365-1609(97)80069-X.

Hoek, E., Carranza-Torres, C. and Corkum, B. (2002), "Hoek-Brown failure criterion – 2002 Edition", *Proceedings of the 5th North American Rock Mechanics Symposium and the 17th Tunnelling Association of Canada Conference*, Toronto, Ontario, Canada, July.

Kiru, R. and Madhav, M. (2010), "Response of rigid footing on reinforced granular fill over soft soil", *Geomech. Eng*., **2**(4), 281-302. https://doi.org/10.12989/gae.2010.2.4.281.

Kuo, Y.L., Jaksa, M.B., Lyamin, A.V. and Kaggwa, W.S. (2009), "ANN-based model for predicting the bearing capacity of strip footing on multi-layered cohesive soil", *Comput. Geotech*., **36**(3), 503-516. https://doi.org/10.1016/j.compgeo.2008.07.002.

Lyamin, A.V. and Sloan, S.W. (2002), "Lower bound limit analysis using non-linear programming", *Int. J. Numer. Meth. Eng*., **55**(5), 573-611. https://doi.org/10.1002/nme.511.

Lyamin, A.V. and Sloan, S.W. (2002), "Upper bound limit analysis using linear finite elements and non-linear programming", *Int J Numer. Anal. Meth. Geomech*., **26**(2), 181-216. https://doi.org/10.1002/nag.198.

Marinos, P. and Hoek, E. (2001), "Estimating the geotechnical properties of heterogenous rock masses such as flysch", *Bull. Eng. Geol. Environ*., **60**(2), 85-92. https://doi.org/10.1007/s100640000090.

Marinos, P., Hoek, E. and Marinos, V. (2006), "Variability of the engineering properties of rock masses quantified by the geological strength index: The case of ophiolites with special emphasis on tunneling", *Bull. Eng. Geol. Environ*., **65**(2), 129-142. https://doi.org/10.1007/s10064-005-0018-x.

Marinos, V. and Carter, T.G. (2018), "Maintaining geological reality in application of GSI for design of engineering structures in rock", *Eng. Geol*., **239**, 282-297. https://doi.org/10.1016/j.enggeo.2018.03.022.

Merifield, R.S., Lyamin, A.V. and Sloan, S.W. (2006), "Limit analysis solutions for the bearing capacity of rock masses using the generalised Hoek-Brown criterion", *Int. J. Rock Mech. Min. Sci*., **43**(6), 920-937. https://doi.org/10.1016/j.ijrmms.2006.02.001.

Meyerhof, G.G. (1951), "The ultimate bearing capacity of foundations", *Geotechnique*, **2**(4), 301-332. https://doi.org/10.1680/geot.1951.2.4.301

Meyerhof, G.G. (1974), "Ultimate bearing capacity of footings on sand layer overlying clay", *Can. Geotech. J*., **11**(2), 223-229. https://doi.org/10.1139/t74-018.

Misir, G. and Laman, M. (2016), "A modern approach to estimate the bearing capacity of layered soil", *Period. Polytech. Civ. Eng*., **61**(3), 434-446. https://doi.org/10.3311/ppci.9578.

Okamura, M., Takemura, J. and Kimura, T. (1998), "Bearing capacity predictions of sand overlying clay based on limit equilibrium methods", *Soils Found*., **38**(1), 181-194. https://doi.org/10.3208/sandf.38.181.

Özbek, A. and Gül, M. (2014), "The geotechnical evaluation of sandstone-claystone alternations based on geological strength index", *Arab. J. Geosci*., **8**(7), 5257-5268. https://doi.org/10.1007/s12517-014-1541-5

Santa, C., Gonçalves, L. and Chaminé, H.I. (2019), "A comparative study of GSI chart versions in a heterogeneous rock mass media (Marão tunnel, north Portugal): A reliable index in geotechnical surveys and rock engineering design", *Bull. Eng. Geol. Environ*., **78**(8), 5889-5903. https://doi.org/10.1007/s10064-019-01481-7.

Satyanarayana, B. and Garg, R.K. (1981), "Bearing capacity of footings on layered C-PHI soils", Technical note, *Int. J. Rock Mech. Min. Sci. Geomech. Abstr*., **18**(1), 14. https://doi.org/10.1016/0148-9062(81)90444-7.

Serrano, A. and Olalla, C. (1994), "Ultimate bearing capacity of rock masses", *Int. J. Rock Mech. Min. Sci. Geomech. Abstr*., **31**(2), 93-106. https://doi.org/10.1016/0148-9062(94)92799-5.

Serrano, A., Olalla, C. and González, J. (2000), "Ultimate bearing capacity of rock masses based on the modified Hoek-Brown criterion", *Int. J. Rock Mech. Min. Sci*., **37**(6), 1013-1018. https://doi.org/10.1016/S1365-1609(00)00028-9.

Shahin, M.A. and Cheung, E.M. (2011), "Stochastic design charts for bearing capacity of strip footings", *Geomech. Eng*., **3**(2), 153-167. https://doi.org/10.12989/gae.2011.3.2.153.

Shoaei, M.D., Alkarni, A., Noorzaei, J., Jaafar, M.S., Bujang, B. and Huat, K. (2012), "Review of available approaches for ultimate bearing capacity of two-layered soils", *J. Civ. Eng. Manage*., **18**(4), 469-482. https://doi.org/10.3846/13923730.2012.699930.

Sloan SW. (1988), "Lower bound limit analysis using finite elements and linear programming", *Int. J. Numer. Anal. Meth. Geomech*., **12**(1), 61-77. https://doi.org/10.1002/nag.1610120105.

Sloan, S.W. and Kleeman, P.W. (1995), "Upper bound limit analysis using discontinuous velocity fields", *Comput. Meth. Appl. Mech. Eng*., **127**(1-4), 293-314. https://doi.org/10.1016/0045-7825(95)00868-1.

Sokolovskii, VV. (1965), *Statics of Soil Media*, Butterworths Science, London, U.K.

Tajeri, S., Sadrossadat, E. and Bazaz, J.B. (2015), "Indirect estimation of the ultimate bearing capacity of shallow foundations resting on rock masses", *Int. J. Rock Mech. Min. Sci*., **80**, 107-117. https://doi.org/10.1016/j.ijrmms.2015.09.015.

Terzaghi, K. (1943), *Theoretical Soil Mechanics*, Wiley, New York, U.S.A.

Uncuoğlu, E. (2015), "The bearing capacity of square footings on a sand layer overlying clay", *Geomech. Eng*., **9**(3), 287-311. https://doi.org/10.12989/gae.2015.9.3.287.

Zhu, M. (2004), "Bearing capacity of strip footings on two-layer clay soil by finite element method", *Proceedings of the 2004 ABAQUS Users' Conference*, Boston, Massachusetts, U.S.A., May.

CC